2023

TiO2-MWCNT Nanohybrid: Cytotoxicity, protein corona formation and cellular internalisation in RTG-2 fish cell line

Gabriela Helena Da Silva
Brazilian Nanotechnology National Laboratory, Brazil

Lidiane Silva Franqui
Brazilian Nanotechnology National Laboratory, Brazil

Marcelo A. De Farias
Brazilian Nanotechnology National Laboratory, Brazil

See next page for additional authors

Funder: Government of Ireland International Education Scholarship (GOI-IES), the National Council for Scientific and Technological Development (CNPq), the Coordenação de Aperfeiçoamento de Pessoal de Nível Superior (CAPES/ Brasil) finance code 001, the National System of Laboratories on Nanotechnologies (SisNANO/MCTIC), the National Institute of Science, Technology and Innovation for Functional Complex Materials (INTC-Inomat) and the São Paulo

TiO_2-MWCNT nanohybrid: Cytotoxicity, protein corona formation and cellular internalisation in RTG-2 fish cell line

Gabriela H. Da Silva[1,2,3,4*], Lidiane Silva Franqui[1], Marcelo A. De Farias[1], Vera Lucia S. S. De Castro[3], Hugh J. Byrne[4], Diego S. T. Martinez[1,2], Regina T. R. Monteiro[2], and Alan Casey[4]

[1]Brazilian Nanotechnology National Laboratory (LNNano), Brazilian Center for Research in Energy and Materials (CNPEM), Campinas, São Paulo, Brazil

[2]Center of Nuclear Energy in Agriculture (CENA), University of São Paulo (USP), Piracicaba, São Paulo, Brazil

[3]Laboratory of Ecotoxicology and Biosafety, EMBRAPA Environment, Jaguariúna, São Paulo, Brazil

[4]FOCAS Research Institute, TU Dublin, City Campus, Camden Row, Dublin 8, Ireland

[*]Corresponding author: gabriela.silva@lnnano.cnpem.br

Abstract

Titanium dioxide nanoparticles-multiwalled carbon nanotubes (TiO_2-MWCNT) nanohybrids have enhanced photocatalytic activity across visible light with promising applications in environmental remediation, solar energy devices and antimicrobial technologies. However, little is known about the toxicological properties of TiO_2-MWCNT. In this sense, it is necessary to evaluate the toxicological effects of TiO_2-MWCNT towards the safe and sustainable development of nanohybrids. In this work, we studied the cytotoxicity, protein corona formation and cellular internalisation of TiO_2-MWCNT on fibroblasts derived from gonadal rainbow trout tissue (RTG-2) for the first time. This nanohybrid did not show any toxic effect on RTG-2 cells up to 100 µg mL^{-1} after 24 h of exposure as monitored by alamar blue, neutral red and trypan blue assays (in the presence or absence of fetal bovine serum, FBS). Furthermore, cryo-transmission electron microscopy analysis demonstrated that TiO_2 particles were attached to the surface of nanotubes after FBS-protein corona formation in a cell culture medium. Raman spectroscopy imaging showed that TiO_2-MWCNT could be internalised by RTG-2 cells. This work is a novel contribution towards better understanding the nano-bio interactions of nanohybrids linked to their in vitro effects on fish cells in aquatic nanoecotoxicology.

Keywords: Nanosafety, Protein corona, Raman, Ecotoxicity.

1. Introduction

Nanohybrid materials have been attracting increasing attention for health, energy and environmental (Belkhanchi et al., 2021, 2020; Sharma et al., 2021; Yoon et al., 2021). Combining two or more nanomaterials (NMs) to form nanohybrids can generate new functionalities and/or enhanced properties (Saleh et al., 2014). In this sense, the combination of titanium dioxide nanoparticles (TiO_2) and multi-walled carbon nanotubes (MWCNT) is particularly interesting in producing a nanohybrid material. TiO_2 is a widely used nanoparticle with low synthesis cost, high photostability and photocatalytic activity (Nasr et al., 2018). Due to its large band gap (3.3 eV), this particle only absorbs in the near UV region. Therefore, there has been an intensive effort to reduce the bandgap of TiO_2 so that it absorbs in visible regions of the spectrum (Hernández-Alonso et al., 2009). MWCNTs have good mechanical stability, electronic properties, and large surface area, acting as electron donor and enhancing the photocatalytic activity of TiO_2 (Olowoyo et al., 2019; Sharma et al., 2021). In this context, the combination of TiO_2 and carbon nanotubes creates a composite with an increased photocatalytic activity, extended to visible light (Da Dalt et al., 2013; Da Silva et al., 2018; Hemalatha et al., 2015; Nasr et al., 2018). Consequently, this nanohybrid shows promising properties, especially for environmental applications, in which it has been demonstrated to be efficient for the degradation of several dyes and pollutants (Chen et al., 2011; Da Silva et al., 2018; Hamid et al., 2014; Zhao et al., 2010; Zouzelka et al., 2016). Besides, it can also be applied for energy storage (Guler et al., 2015; Mombeshora et al., 2022), photovoltaic energy conversion (Muduli et al., 2009; Wang et al., 2015), renewable energy (Lee et al., 2007; Muduli et al., 2009), sensors (Chen et al., 2022; Sánchez et al., 2007), bactericidal activity (W. Oh et al., 2009), among others.

Although nanohybrid production and technology can bring many benefits, as the particles present new and enhanced properties, the impact on the environment or human health may differ from that of the constituent components. Therefore, the safe-by-design approach, including a minimum amount of information about the material's physical-chemical properties, such as size distribution, morphology and surface charge, colloidal behaviour, like aggregation and sedimentation, and toxicity assessment, are crucial towards a safe application and commercialisation of these materials. This approach steps

forward to a sustainable and responsible nanotechnology innovation, preventing hazardous impacts on human and environmental health (de Medeiros et al., 2021).

TiO_2-MWCNT synthesis, characterisation, and toxicity evaluation towards zebrafish embryos have previously been reported by our research group (Da Silva et al., 2018). This nanohybrid was synthesised with an easy and eco-friendly technique and proved safe for zebrafish embryo development. However, micro-X-ray fluorescence indicated the ingestion of the material by embryos, which may cause effects at the cellular level. Fundamentally, all toxicological responses are related to an impairment of some aspect of cellular activity, for example, cellular uptake, effects on cell signalling, membrane perturbations, production of cytokines, chemokines, ROS, cell necrosis or apoptosis, among others. Those responses often reflect on some physiologic responses observed during *in vivo* testing. Hence, in some cases, *in vitro* assays present a reasonable correlation with *in vivo* (Bols et al., 2005; Di Ianni et al., 2021; Jones and Grainger, 2009; Scott et al., 2021). Another advantage is that *in vitro* tests allow an extensive screening of effects using a small amount of material. Besides, it can be used as an alternative for *in vivo*, relying on the principle of the "3R" aiming to Reduce, Refine and Replace animal experiments (Forest, 2022; Quevedo et al., 2021).

Fibroblasts derived from gonadal rainbow trout tissue (RTG-2) is a fish cell line commonly used in aquatic toxicity evaluations. The *in vitro* test with this cell line can be proposed as an alternative method for risk assessment studies, being proven to have a reasonable correlation with *in vivo* fish testing (Castaño et al., 1996; Kolarova et al., 2021). A wide range of cytotoxicity standard tests can be performed with this cell line, such as tetrazolium salt reduction (MTT), alamar blue (AB) and neutral red (NR) assays (Fent, 2001; Hernández-Moreno et al., 2022), allowing a fast obtention of a considerable amount of data, ranging from cell metabolic activity, cell membrane integrity, mitochondria toxicity, lysosome toxicity, etc. Thus, this cell line is being extensively used to understand the toxic mechanisms of environmental contaminants. The obtained results can be used to determine the toxicological profile of chemical modes of toxic action, such as oxidative damage, genotoxicity, membrane disruption, and apoptosis, among others. Therefore, the RTG-2 cell line has been extensively used for nanotoxicity studies (Bermejo-Nogales et al., 2017; Casado et al., 2013; Goswami et al., 2022; Klingelfus et al., 2019; Munari et al., 2014; Vevers and Jha, 2008).

It is a consensus that the behaviour of NMs in a biological environment (e.g., colloidal stability, aggregation, sedimentation, adsorption of biomolecules, surface charge) plays a crucial role in nanotoxicology (da Cruz Schneid et al., 2022; Nel et al., 2009; Petry et al., 2019). When in a biological environment, NMs interact with the biomolecules forming a coating on its surface, commonly referred to as a protein corona (when the biomolecules adsorbed are mainly proteins) or biomolecular corona (Monopoli et al., 2012; Paula et al., 2014). Environmental dimensions of protein coronas have been recently considered, showing critical implications for nanoecotoxicology (Wheeler et al., 2021). In fact, the corona formation confers a new biological and ecological identity to nanomaterials that strongly impact their interactions with living organisms and the environment, critically influencing nanomaterial uptake, biodistribution and toxicity (Martinez et al., 2020; Martins et al., 2022; Morozesk et al., 2018; Natarajan et al., 2021). The corona formation can occur not only in the environment but also under controlled experimental conditions, where the presence of biomolecules, such as fetal bovine serum proteins (FBS) present in the cell culture medium, can modulate the toxicological response. Therefore, it is imperative to study the interaction of nanomaterial-corona to understand the toxicological results obtained in nanotoxicological studies. To the best of our knowledge, there are no reports in the literature considering the protein corona formation on TiO_2-MWCNT linked to its toxicity in RTG-2 fish cells.

In this work, we studied the cytotoxicity and cellular internalisation of TiO_2-MWCNT nanohybrid on RTG-2 cells, considering the influence of protein corona formation. We have applied an integrated approach using advanced microscopy techniques such as cryogenic transmission electron microscopy, enhanced dark-field hyperspectral microscopy and Raman microspectroscopy to better understand nano-bio interactions, such as protein corona and nanomaterial-cell interactions. Also, we applied an *in vitro* toxicity assessment towards alternative methods in aquatic toxicology and nanosafety research.

2. Materials and methods

2.1. TiO_2-MWCNT nanohybrid material

The TiO_2-MWCNT sample used in the present study was previously synthesised and characterised, as reported by Da Silva et al. (2018). Briefly, this sample was prepared

by mechanical milling methods from a proportion of 10:3 of TiO_2 (P25 – Degussa Evonik, Essen, Germany) and MWCNT (CNT Co. Ltd). Prior to the experiments, the TiO_2-MWCNT stock dispersion (0.5 mg mL^{-1}) was prepared in ultrapure water by sonication for 1 h in an ultrasonic bath (Cole-Parmer, model 08895-43, USA) and then stored, protected from light, at room temperature until further use.

2.2. Dispersion stability and Cryo-TEM analysis

Colloidal stability studies of TiO_2-MWCNT at a concentration of 100 μg mL^{-1} in DMEM, with and without the addition of 10% FBS, were performed with a spectrophotometer (Multiskan GO, Thermo Scientific, UK) by measuring the optical density at 350 nm after 0, 1, 4 and 8 and 24 hours. A Zetasizer Nano ZS90 instrument (Malvern Instruments, UK) was used to evaluate the hydrodynamic diameter (HD) and polydispersity index (PDI) through dynamic light scattering (DLS) and Zeta potential (ZP) by electrophoretic light scattering (ELS). For DLS measurements, all samples were measured using the "General purpose" analysis method at a scattering angle of 173° (backscatter) and the default size analysis parameters as well as a refractive index of 1.59 for the polystyrene particle matrix as sample parameter. The obtained results were the intensity-weighted harmonic mean particle diameter (Z-Average) and the polydispersity index (PI). For electrophoretic mobility measurements from which zeta potential is deduced, the approximation of Smoluchowski was carried out at a temperature of measurement of 25.0 °C by ELS, voltage selection and attenuation selection were set in the automatic mode, except for stability studies with FBS where the voltage was set for 10 V. All analyses were performed in triplicate.

Cryo-transmission electron microscopy (Cryo-TEM) was used to determine the synthesis efficiency and evaluate whether the combination of TiO_2 and MWCNT remained intact in the cell culture medium (Dulbecco's modified nutrient medium - DMEM). More traditional TEM preparation techniques demand drying or plastic embedding of the sample. Hence, the sample sometimes corresponds to a distorted version of the original. Cryo-TEM sample preparation is by freezing, this way, images can be generated in a real state of hydration of the sample, which is essentially how it exists in solution, avoiding sample deformation by the microscope vacuum and drying effect. Samples containing 100 μg mL^{-1} of TiO_2-MWCNT in ultrapure water and DMEM,

with and without 10% fetal bovine serum (FBS) supplementation, were prepared using a Vitrobot Mark IV specimen preparation unit (Thermo Fischer Scientific, USP). The analysis was performed using the transmission electron microscope (TEM) TALOS F200C (Thermo Fischer Scientific, USA) operating at 200 kV. The images were acquired using a Ceta 16M CMOS camera with 4k by 4k pixels (Thermo Fisher Scientific, USA). The hole grid was analysed for all samples, and two individual analyses were performed. The sample was assessed visually, and no statistical analyses were performed.

2.3. Protein corona characterisation

The interaction between the FBS proteins and TiO_2-MWCNT was evaluated by SDS-PAGE gel analysis. Protein corona formation is a highly dynamic process, and its composition may change over time. However, studies have shown that protein corona and their composition are established rapidly (Tenzer et al., 2013). Most studies have revealed that hard corona remains stable after 1 hour of incubation (Docter et al., 2014; Franqui et al., 2019; Lesniak et al., 2012; Lundqvist et al., 2011; Martins et al., 2022). However, to show that for TiO_2-MWCNT 1 hour of incubation was enough to achieve the equilibrium of protein adsorption, we performed the protein incubations with 1 and 24 hours. Briefly, the protein corona was prepared by incubating 100 μg mL^{-1} of TiO_2, MWCNT and TiO_2-MWCNT in DMEM supplemented with 10% of FBS for 1 and 24 hours at 22°C. The temperature was chosen because all cytotoxicity assays were performed at 22°C. After incubation, the dispersion was centrifuged at 20817 g for 1 h at 4°C, followed by three washes with PBS (centrifuging for 30 min at 4°C and 20817 g, discarding the supernatant) for removal of poorly bound and unbound proteins. The pellet obtained, formed by the nanomaterial and strongly bound proteins (hard corona), was resuspended in 100 μL of deionised water and sonicated for 2 min. To extract the proteins, 40 μl of sample buffer and 10 μl of dithiothreitol (DTT) 1:10 were added, followed by another sonication step (2 min), after which the samples were incubated at 99 °C for 3 min. Finally, 15 μl of the sample was loaded onto 15% SDS-PAGE gel (Franqui et al., 2019).

2.4. RTG-2 cell line culture conditions

Cell lines derived from fish are widely used for the cytotoxic analysis of environmental contaminants (Galbis-Martínez et al., 2018; Lungu-Mitea et al., 2018;

Yurdakök-Dikmen et al., 2018) and nanoparticles (Casado et al., 2013; Morozesk et al., 2020; Naha et al., 2009; Naha and Byrne, 2013). Hence, Rainbow trout gonadal tissue cell line (RTG-2) lineage was used for *in vitro* evaluation of TiO_2-MWCNT cytotoxicity assay. This cell line was provided by the Dublin Institute of Technology, FOCAS Research Institute, Ireland. Cells were maintained in DMEM (high glucose and pyruvate; ThermoFisher, USA) supplemented with 10% FBS (sterile, heat-inactivated and free from mycoplasma, Cultilab, Brazil), 100 IU mL^{-1} penicillin, 100 μg mL^{-1} streptomycin, and 25 mM 4-(2-hydroxyethyl)-1-piperazineethanesulfonic acid (HEPES). Cultures were maintained in an incubator at 22 ± 1 °C under a normal atmosphere and sub-cultured upon reaching 80% confluence.

2.5. Cellular viability assays

Most colorimetric cell viability assays, which verify cell viability by assessing plasma and lysosomal membrane integrity, such as the trypan blue and neutral red assays, respectively, or assess the metabolic activity of cells, such as MTT and alamar blue, can interact with NPs (Breznan et al., 2015; Casey et al., 2007), culminating in false results. Therefore, the use of more than one type of cytotoxicity assay is recommended. For this reason, three standard viability tests, alamar blue, neutral red and trypan blue, were employed to increase data reliability. Besides a NM adsorption, with alamar blue and neutral red without the cells was performed to analyse if nanomaterials were interfering with the cytotoxicity assay. Results are shown in the supplementary material.

2.5.1. Alamar blue

Cell viability was analysed by the alamar blue (AB) assay, which has been extensively used as an indicator of the cytotoxicity of nanomaterials. AB fluorometric assay is based on the nonspecific, enzymatic, irreversible reduction of the resazurin compound to resorufin by viable cells (MITJANS, 2018). Briefly, 96-well cell culture plates (Flat Bottom, TC Treated, sterile – NEST) were seeded with a cell density of $2x10^5$ cells per mL and allowed to attach overnight. Subsequently, serial dilutions of TiO_2-MWCNT in DMEM (concentration ranging from 0.078 to 100 mg L^{-1}), with and without the addition of 10% FBS, were added and the plates were incubated for 24 hours, at 22 ± 1 °C under normal atmosphere. After the exposure, cells were washed with sterile phosphate buffered saline (PBS) and incubated for 3 hours at 22°C with 100 μL of DMEM

containing 10% of alamar blue reagent. Fluorescence was measured using an excitation wavelength of 530 nm and an emission wavelength of 595 nm on a multi-plate reader (Spectra Max—M3).

2.5.2. Neutral red

Neutral Red (NR) is an indicator of cell survival based on the ability of viable cells to incorporate and retain NR dye in the lysosomes. Toxic substances cause a decrease in NR uptake, such that spectrophotometric measurements indicate cell viability (BOLS et al., 2005). The exposure was done similarly to alamar blue. After exposure, cells were washed with PBS and incubated for 3 hours at 22 °C with 100 µL of DMEM containing 1.25 µL of NR stock (4 mg mL^{-1}). After incubation, cells were washed with PBS, and 150 µl of the reaction solution (1% acetic acid, 50% ethanol and 49% distilled water) was added. The plate was shaken for 10 min at 240 rpm, and then the absorbance at 540 nm was recorded (Multiskan GO, Thermo Scientific, UK).

2.5.3. Trypan blue

Colorimetric assays can often lead to false results in NM cytotoxicity assays (CASEY et al, 2007). Thus, trypan blue viability assay was used as an alternative to colorimetric assay. The principle of this assay is that living cells with intact cell membranes exclude the trypan blue stain, whereas dead cells do not. Hence, the trypan blue assay consists of a simple assay to determine the number of viable cells in a cell suspension (Stone, Johnston, & Schins, 2009). $2x10^5$ cells per mL were platted in a 96-well plate and allowed to attach overnight. Cells were then exposed to 1, 10 and 100 mg L^{-1} of TiO_2-MWCNT in DMEM (with and without 10% FBS) for 24h at 22 °C. Subsequently, cells were washed with PBS, and 30 µL of trypsin was added to each well, after 5 minutes 100 µL of DMEM were added, and the suspension was centrifuged for 1 min at 1500 rpm. The pellet was resuspended in 10 µL of DMEM and 10 µL of trypan blue reagent. Cells were counted in a Neubauer chamber, and cell numbers were calculated.

2.6. Cell cycle

Cell cycle studies were performed to determine whether there were any differences between the cyclic behaviour of the cells. Briefly, to monitor the cell cycle, cells were seeded in T-25 cm^2 flasks at a density of 2×10^6 cell per mL (5 mL of DMEM) and allowed to attach overnight. Subsequently, cells were exposed for 24 hours (in at

normal atmosphere and 22 °C) to 1 mg L^{-1} of TiO_2-MWCNT (higher concentrations caused clumping of cells, interfering with the analysis). After exposure, the cells were washed with PBS three times and harvested by enzymatic removal (trypsin). They were fixed in 70% ethanol for 30 minutes, centrifuged (1400 rpm) for 5 minutes and washed with PBS twice. Next, cells were treated with 100 µg mL^{-1} of ribonuclease for 5 min, stained with 50 µg mL^{-1} propidium iodide and incubated for 20 min, after which they were immediately analysed. A minimum of 10,000 single-cell events per sample were analysed with a BD AccuriTM C6 Flow Cytometer.

2.7. Enhanced dark-field hyperspectral microscopy

RTG-2 cells were seeded on common microscopy coverslips at a density of $1x10^5$ cells per coverslip in 3 mL of DMEM supplemented with 10% FBS and allowed to attach overnight. The coverslips were placed in a 6-well plate and pre-treated with a 1% gelatine solution to increase cell adhesion. After this period, cells were exposed for 24 hours to 1 mg L^{-1} of TiO_2-MWCNT in DMEM, with and without FBS supplementation (10%). Subsequently, cells were washed three times with PBS and fixed with glutaraldehyde (2%). For the analysis, cells were kept in ultrapure water. An Olympus microscope (BX-53, Japan) coupled with a VNIR hyperspectral camera (Cytoviva, Inc., Alabama) and a high-resolution dark field capacitor (numerical aperture; NA 1.2-1.4) were used. This system provides a resolution of 90 nm, with excellent contrast and signal-to-noise ratio. Samples were analysed using a 100x immersion objective (Olympus UPlanFLN 100x, 1.3 NA). Conventional dark-field images were collected with a Dagexcel-M camera (Dage-MTI, Michigan, IN). The spectral images were analysed using ENVI 4.8 software. The software tool "filter particle" was used to avoid false positives, which removed all control spectra from the treatment. In this way, the spectra present in the map corresponded only to the NM spectra.

2.8. Raman microspectroscopy

To evaluate whether the TiO_2-MWCNT had the potential of cellular internalisation, Raman microspectroscopy was used. For this analysis, RTG-2 cells were seeded on calcium fluoride (CaF_2) discs at a density of $2x10^5$ cells per disc with 3 mL of DMEM supplemented with 10% FBS and allowed to attach overnight. Subsequently, they

were exposed for 24 hours to 1 mg L^{-1} of TiO_2-MWCNT in DMEM, with and without supplementation of FBS (10%). Afterwards, the medium was removed, cells were washed three times with PBS, fixed with formalin for 3 min and kept in ultrapure water until the analysis. A Horiba Jobin-Yvon LabRAM HR800 spectrometer, equipped with a diode laser with an excitation line at 532 nm, power of 50mW and a 100x immersion objective (LUMPlanF1, Olympus, NA 1.00), was used. The spectrum, from 300 cm^{-1} to 3200 cm^{-1}, was obtained with a grating of 600 lines/mm and a confocal aperture of 100 μm. The Z axis (depth) map was acquired from the cytoplasmic region of 3 different cells for each treatment, with 20 points and 0.5 μm increment, in the Z direction. The acquisition time was 20 seconds.

2.9. Statistical analysis

All tests were performed in triplicates and with three individual repetitions, the statistical analysis was carried out using OriginPro 2022 software (OriginLab). All data were tested for normality using the Kolmogorov_Smirnov test and for homogeneity of variance by Brown-Forsythe test. If parameter assumptions of normal distribution and homogeneity of variance were met, ANOVA was followed by Dunnet's test to compare the data. Where the assumptions were not met, data were analysed using the nonparametric Kruskas-Wallis ANOVA followed by Dunn's test of multiple comparisons.

3. Results and discussion

Accurate characterisation of the NM state in the biological medium is essential to determine their potential adverse effects. The colloidal stability of the TiO_2-MWCNT dispersion in Dulbecco's Modified Eagle's Medium (DMEM), with and without the addition of fetal bovine serum (FBS) (10%), was evaluated by ultraviolet-visible spectroscopy (UV-vis) (Figure 1), indicating the loss of absorbance as a function of time due to sedimentation. Hydrodynamic diameter, polydispersity index (PDI) and zeta potential were analysed by dynamic light scattering (DLS) and electrophoretic light scattering (ELS) measurements (Zetasizer, Malvern Instrument) (Table 1). In ultrapure water and DMEM, TiO_2-MWCNT was highly unstable, resulting in agglomeration and sedimentation (Figure 1). Since oxygenated groups are responsible for promoting the

colloidal stability of oxidised multiwalled carbon nanotubes (ox-MWCNT), the low stability of this nanomaterial may be a consequence of TiO_2 binding to these groups. Besides, the media salts facilitate counter ion migration into the solvation layer of nanoparticles decreasing electrostatic forces, also a elevate ionic strength in media can increase Van der Waals force of attraction between particles, this increases aggregation and sedimentation of particles (Das et al., 2022; Parsai and Kumar, 2019). Similar behaviour was observed by Das et al. (2018) when studying the stability of TiO_2-MWCNT. In their studies, it was concluded that the degree of aggregation increased according to increased amounts of TiO_2 in the sample and, consequently, a smaller amount of oxygenated groups available in the MWCNT structure. For TiO_2 nanoparticles, aggregation and sedimentation were also observed when particles were dispersed in DMEM. However, in the presence of proteins, a decrease in both parameters was observed. The same was also observed for carbon nanotubes (CNTs), as several studies have already shown that serum proteins are adsorbed by CNTs, promoting steric stabilisation of the dispersion, reducing the rate of aggregation in biological media (Du et al., 2014; Sacchetti et al., 2013; Wang et al., 2010). In our study, TiO_2-MWCNT exhibited a smaller hydrodynamic size in DMEM with FBS. Hence, FBS proteins cause a decrease in aggregation. However, comparing DLS and UV-Vis data, it is possible to infer that the presence of FBS did not prevent sedimentation but only inhibited aggregation. The same was observed by Allegri et al. (2016) when studying the stability of ox-MWCNT in a protein-rich medium, they observed that, even though ox-MWCNT adsorb a large amount of proteins, they still precipitated over time, consistent with our studies.

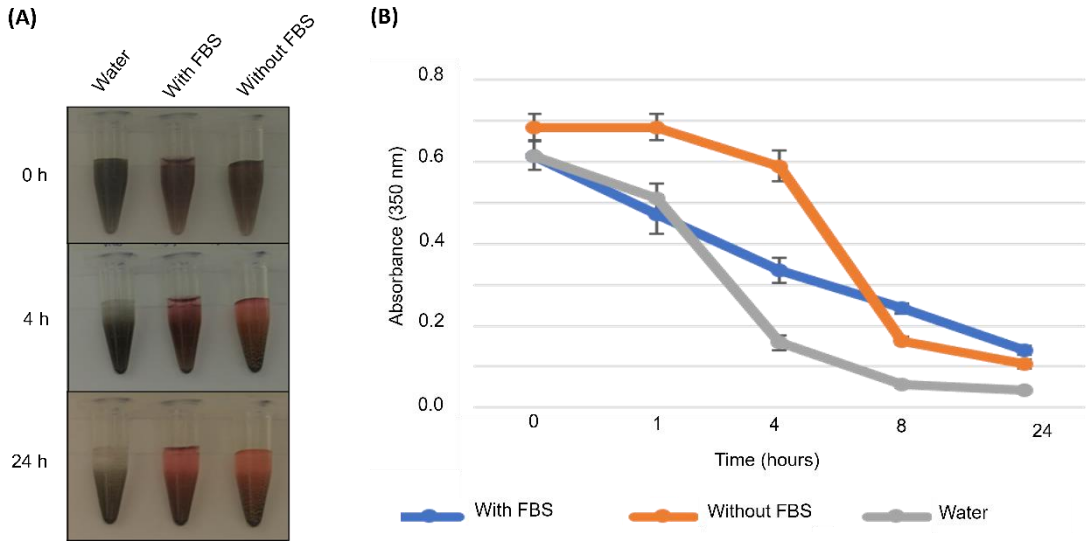

Figure 1. Stability of TiO_2-MWCNT hybrid nanomaterial in DMEM (with and without the addition of FBS) and ultrapure water for 24 hours. (A) TiO_2-MWCNT Dispersion photograph after 0, 4 and 24h in static conditions (water, media without FBS and media with FBS) and (B) UV-Vis absorbance, of the TiO_2-MWCNT, at 350 nm after 0, 1, 4, 8 and 24 hours in static conditions (water, media without FBS and media with FBS).

Table 1. Polydispersity index (PdI) and zeta potential (ZP) of TiO_2-MWCNT suspensions in ultrapure water, DMEM with and without FSB, hydrodynamic diameter (± standard deviation) obtained using DLS and ELS.

Medium	Hydrodynamic diameter (d.nm)	PdI	ZP (mV)
Ultrapure water	741.9 ± 91.6	0.632 ± 0.015	-4.2 ± 0.1
DMEM without FBS	2274.0 ± 337.5	0.683 ±0.185	-12.9 ± 0.7
DMEM with FBS	564.8 ± 51.2	0.646 ± 0.514	-9.0 ± 0.3

To analyse whether DMEM and/or FBS proteins can modify the morphological characteristics of TiO_2-MWCNT, Cryo-TEM was applied. This technique allowed the *in situ* observation of TiO_2-MWCNT in DMEM (with and without FBS supplementation). Our results showed that in all conditions, it was possible to observe tangles of TiO_2-MWCNT, corroborating with the stability results, showing the aggregated state of the materials. Also, it is important to notice that TiO_2 remain bound/attached to TiO_2-MWCNT complex surface in all media conditions, and no free TiO_2 was observed through the Cryo-TEM analysis (Figure 2). These results showed that mechanically milling TiO_2 and MWCNT generate a stable hybrid nanomaterial, as the TiO_2 is strongly

bound to MWCNT surface. Besides is important to highlight the applicability of the Cryo-TEM to study nanoparticles organisation and structure in biological media in nanobiotechnology and nanotoxicity evaluations.

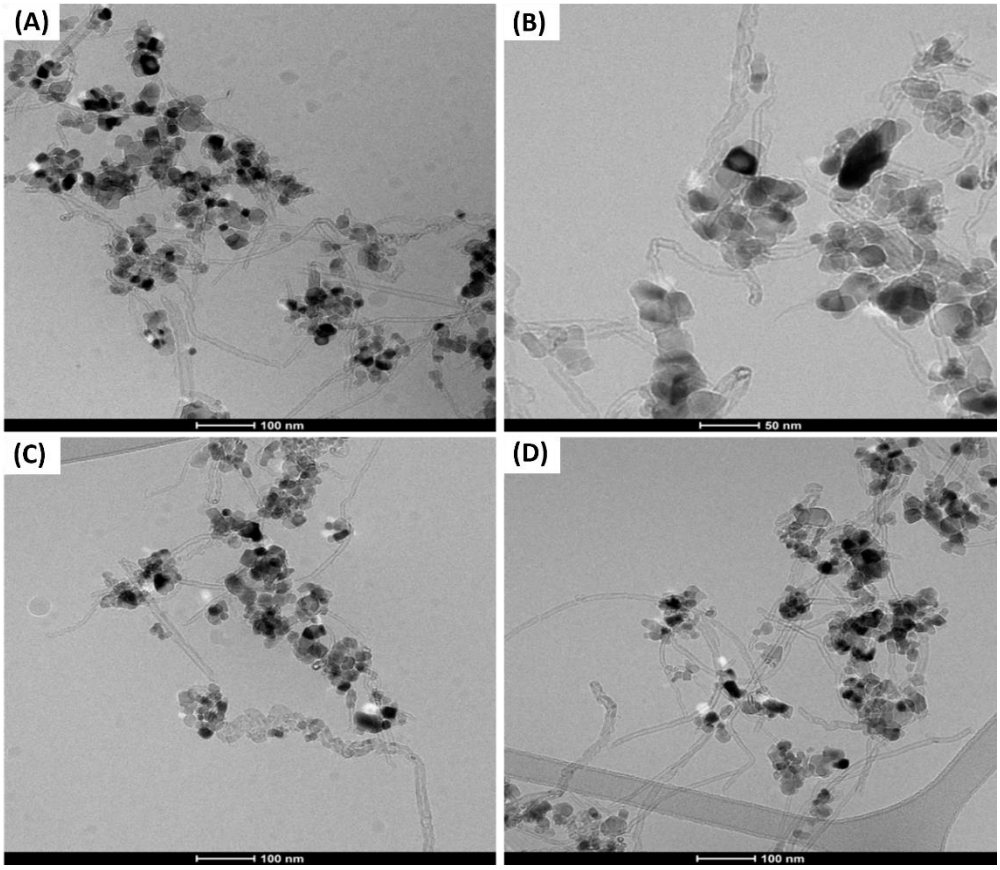

Figure 2. Cryogenic transmission electron microscopy (Cryo-TEM) images of TiO_2-MWCNT (100 mg L^{-1}) in DMEM with FBS (A and B), without FBS (C) and ultra-pure water (D).

The effect that protein corona coating has on TiO_2 and MWCNT properties and cytotoxicity has already been studied by different authors (Allegri et al., 2016; Borgognoni et al., 2015; Garvas et al., 2015; Long et al., 2018a; Runa et al., 2017; Sit et al., 2019). For example, FBS proteins bound to titanium dioxide nanotubes (TiO_2-NTs) stabilise the dispersion but scavenge photogenerated radicals, preventing the phototoxic effect of UV irradiated TiO_2-NTs, and at low concentrations (1 and 5 μg mL^{-1}) even increasing cell viability for the protein corona coated TiO_2-NTs, as observed by Garvas et al. (2015). Long et al. (2018a) observed that protein corona interaction with pristine and carboxylated MWCNTs causes a change in the diameter and zeta potential of those

materials. In their studies, they also observed that the interaction with bovine serum albumin (BSA) increased the internalisation and reduced cytotoxicity of MWCNTs. To our knowledge, our study is the first study addressing the cytotoxicity of TiO_2-MWCNT considering protein corona formation.

To understand the interaction between proteins and the TiO_2-MWCNT, TiO_2 and MWCNT were individually used as control samples. Our results showed that 1 hour of incubation is sufficient to achieve the adsorptions equilibrium (Figure 3). TiO_2-MWCNT and MWCNT protein corona were similar; for both, well-defined bands can be seen between 245 and 58 kDa, and at 32, 25 and 11 kDa. However, for TiO_2 NP, only a few well-defined bands between 245 and 58 kDa, and 11 kDa can be observed, indicating a low variety of proteins were adsorbed by this material. TiO_2-MWCNT bound a lower amount of proteins than MWCNT, but a larger variety than TiO_2. Consequently, the formation of TiO_2-MWCNT hybrid reduced the adsorption of proteins, which can be attributed to the binding of the TiO_2 to the sites used in the protein's interaction with MWCNT.

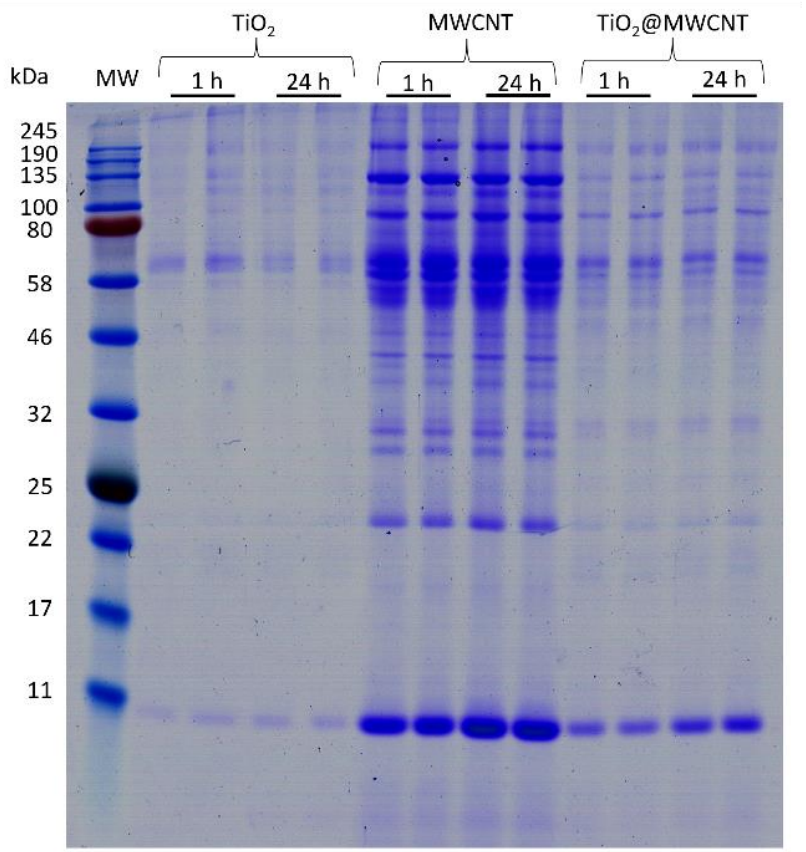

Figure 3. Biochemical characterisation of FBS hard corona associated with TiO_2, MWCNT and TiO_2-MWCNT after incubation of 100 mg L^{-1} of each NM in DMEM with 10% FBS for 1 and 24 hours at 22 °C. MW = molecular weight of protein standard, ranging from 11-245 kDa.

Overall, TiO_2-MWCNT did not elicit cytotoxic responses either with or without FBS, at a concentration ranging from 0 to 100 µg mL^{-1}, after 24 hours of exposure, as monitored by the alamar blue, neutral red and trypan blue assays (Figure 4). David et al. (2022) also studied the cytotoxicity of TiO_2-MWCNT, in their studies the results showed that cellulose acetate-collagen films containing 0.05 g of TiO_2-MWCNT nanoparticles enhanced HDFn cell proliferation at 48 hours of exposure, this material also showed good antimicrobial propriety being an excellent candidate to be applied in biomedical technologies. Cendrowski et al. (2014), however, studying the effect of TiO_2-MWCNT on mouse fibroblasts and human liver cells (0 to 100 µg mL^{-1}), observed that concentrations greater than 25 µg mL^{-1} caused a decrease in cell viability after 24 hours of exposure. However, the material studied by these authors differed in TiO_2 percentage (19%) and TiO_2 crystallinity (anatase). In comparison, our material was composed of approximately 70% of a mixture of rutile and anatase forms of TiO_2 NPs (20 and 80%,

418 respectively) (Da Silva et al., 2018). TiO_2 toxicity can be dependent of many
419 characteristics, such as size, morphology, crystallinity (Cai et al., 2011; Gea et al., 2019;
420 Uboldi et al., 2016; Wang and Fan, 2014). For example, Uboldi et al. (2016) studied the
421 cytotoxicity of TiO_2 and found that anatase caused a significantly higher internalisation
422 of anatase TiO_2 NPs in Balb/3T3 fibroblast, while rutile crystalline form induced more
423 cytotoxicity, genotoxicity, and morphological transformation in both cell lines. The same
424 can be said for MWCNT (Hamilton et al., 2013; Kyriakidou et al., 2020; Zhang et al.,
425 2012; Zhou et al., 2017), depending on diameter, length and functional groups. For
426 example, Zhou et al. (2017) studied the cytotoxicity and genotoxicity of pristine and
427 functionalised (-OH and -COOH) MWCNT and observed that even though pristine
428 MWCN caused more cell death, functionalised MWCNT were more genotoxic, besides
429 the presence of BSA on culture media increase cytotoxicity for all materials. Those
430 studies reinforced the dependence of material physical and chemical characteristics in the
431 toxicological profile of nanomaterials.

432 It is important to notice that after 24 hours of exposure to TiO_2-MWCNT an
433 increase in cell proliferation was observed by AB viability test. Two effects could be
434 occurring, the NM can be stimulating cell metabolism or cell proliferation. Several reports
435 sustain that TiO_2 NPs are biocompatible with cells, with a few reporting an enhancement
436 in cell proliferation. For example, Vijayalakshmi et al. (2015) studied the cytotoxicity of
437 TiO_2 NPs on MG63 cell line and observed that for concentrations up to 100 mg L^{-1}, TiO_2
438 NPs improved cell viability, causing cell proliferation when cells were exposed for 24
439 and 48 hours. The same was observed by Sun et al., (2016), their studies have shown that
440 TiO_2-PEG NPs (<100 mg L^{-1}) can increase cell proliferation for HepG2 cells by
441 increasing cell population in the S phase of cell cycle, they also showed that this NPs
442 could aggregate hepatocyte growth factor receptors on the surface of cells which promote
443 cell proliferation. However, these results are not always consistent, as some studies
444 demonstrated that TiO_2 NPs can induce cell cycle arrest, decreasing cell proliferation.
445 This was observed by Chang et al. (2022), who, through a systematic review and meta-
446 analysis of 33 studies, concluded that TiO_2 NPs cause an increased percentage of cells in
447 the sub-G1 phase, consequently causing cell cycle arrest.

448 For MWCNT, the results also are controversial as few studies also showed that
449 MWCNT can cause cell proliferation, inducing cell cycle aberrations (Mihalchik et al.,
450 2015a; Siegrist et al., 2014), while others showed that they could cause cell growth

inhibitions and cell cycle arrest (Ding et al., 2005; Zhang et al., 2011a). For example, nitrogen-doped MWCNT causes proliferation in SAEC cells exposed for 24 hours to concentrations up to 120 mg L^{-1}, they also observed an increase in the G2 phase of the cell cycle (Mihalchik et al., 2015b). Similarly, Siegrist et al. (2014) observed that carboxylated MWCNT caused proliferation on BEAS-2B cell line when exposed to concentrations up to 2.4 µg cm^{-2} for 72 hours, they also observed a significant increase in the S phase when cells were exposed to 24 µg cm^{-2} of carboxylated MWCNT for 24 hours. Zhang et al. (2011) (Zhang et al., 2011b), however, observed that MWCNT cause a dose-dependent decrease in 3T3 cells and human dermal fibroblast viability, which can be related to the dose-dependent increase of cells in the G1 phase and fewer cells in the S and G2/M phase. Similarly, Morozesk at al. (2020) observed that oxidised MWCNT disturb the cell cycle, causing a reduction of cells in the G2/M phase, indicating a G1/S phase block.

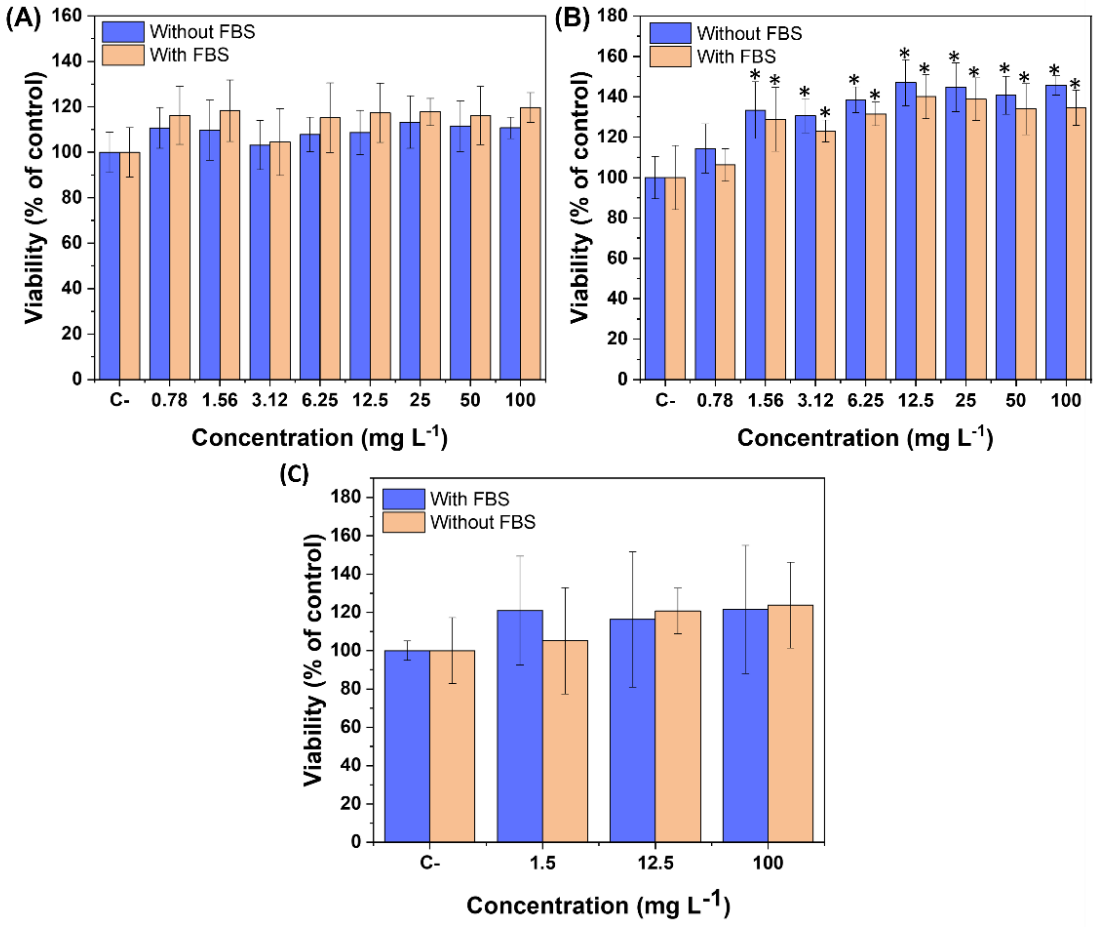

Figure 4. (A) Neutral red, (B) Alamar blue and (C) Trypan blue cell viability assay with RTG-2 cell line exposed to TiO_2-MWCNT for 24 hours. Mean ± SEM of three individual

experiments. Data were analysed by one-way analysis of variance (ANOVA) and post hoc comparisons of mean done by Dunnett's test ($P < 0.05$).

To analyse if the proliferation observed from alamar blue cell viability test was due to cell cycle disruptions, we also performed a cell cycle cytometric flow analysis. Initially, three concentrations were selected for the assay; 1, 10 and 100 mg L^{-1}, although it was only possible to analyse 1 mg L^{-1}. For concentrations of 10 and 100 mg L^{-1}, the NM was seen to be adhered to the cells, forming large aggregates, clogging the instrument and preventing the analysis. No significant results were observed for treatment with FBS compared to the control (Figure 5A). However, a significantly increased G2/M phase of cell division was observed for the treatment without FBS (Figure 5B). In this sense, we hypothesised that cell proliferation occurs in the exposure without FBS supplementation, while an increase in metabolic activity occurs in the exposure with FBS supplementation. Nanomaterials have the ability to increase cell metabolism resulting in a higher signal in metabolic assays, such as AB and MTT (Longhin et al., 2022). This was observed, for example, by Huang et al. (2009), where a time-dependent increase in MTT signal was obtained when NIH 3T3 and HFW cells were exposed to 50 mg L^{-1} of TiO_2 NP. Similarly, Machado et al. (2019), when studying the toxicity of hydroxyapatite nanoparticles by MTT assay, observed an increase in HDFn cells metabolism after 48 hours of exposure to 320 mg L^{-1} of NP. Dhenge et al. (2020) also observed a higher MTT signal, indicating an increase in metabolism for WJ-MSCs cells exposed to 25 and 10 mg L^{-1} of hybrid graphene oxide.

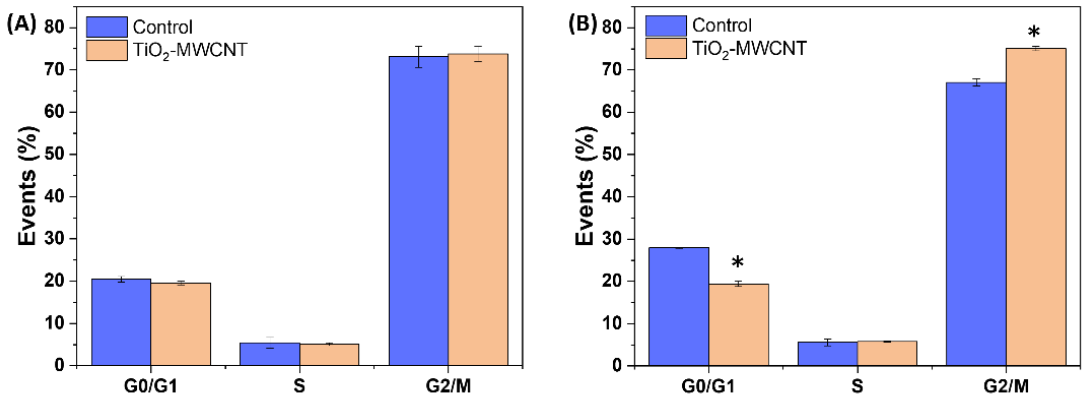

Figure 5. Cell cycle cytometric flow assay with RTG-2 exposed to 1 mg L^{-1} of TiO_2-MWCNT for 24 hours (A) with and (B) without FBS in DMEM media. Mean ± SEM of

three individual experiments. Data were analysed by one-way analysis of variance (ANOVA), post hoc comparison of mean done by Dunnett's test (* = $P < 0.05$).

The interaction between nanomaterials and RTG-2 cells was analysed by enhanced dark-field hyperspectral microscopy (CytoViva). Figure 6 A and B show hyperspectral images of the mapped RTG-2 cell, in which the red dots represent the pixels where TiO_2-MWCNT spectra were found. It was observed that, even after several washing steps, NP was still attached to the cell membrane. Hence, to analyse if NP were being internalised, Confocal Raman spectroscopy was applied. Measurements in the Z axis (depth) were used to detect the internalisation of the nanomaterials through the intensity of the MWNT D and G bands measured when translating along the Z axis (1 μm steps) (Alnasser et al., 2019). We can observe that, for TiO_2-MWCNT treated with FBS (Figure 6G), the intensity of the D and G bands was consistently larger inside the cells and that this intensity decreases at the extremes of the Z axis (top and bottom of the cell), proving that the nanomaterial was present inside the cell. In the absence of FBS, the intensity of the D and G bands was highest at the top of the cells but decreased monotonically along the Z axis. Therefore, without FBS, TiO_2-MWCNT tended to aggregate and adhere to the cell membrane. Studies suggested that protein corona can promote nanoparticle uptake. For example, Posati et al. (2012) studied the effect of bovine serum albumin (BSA) in the internalisation of ZnAl-HTlc NP on MDCK and HeLa cell lines and observed that in the presence of BSA the NM was internalised. However, no internalisation was observed in the absence of BSA. For TiO_2 NPs, Tedja et al. (2012) studied the uptake profile of TiO_2 NPs in the presence and absence of serum and observed that in the presence of FBS the uptake of TiO_2 NPs was higher than in non-FBS treated TiO_2 NPs. These results were also observed by Vranic et al. (2017) where TiO_2 NPs in the presence of bovine serum were more efficiently internalised. In the case of MWCNT, Long et al. (2018b) observed that pre-incubation on MWCNT with BSA, forming a protein corona, enhances the internalisation of this material to HUVEC cells. Similarly, Zhang et al. (2019) observed that protein corona-coated pristine MWCNT were more internalised than uncoated pristine MWCNT.

Considering the above, only a limited information is available about the cytotoxicity and internalisation of TiO_2@MWCNT. Hence, this study provides an important contribution towards the toxicological evaluation of TiO_2@MWCNT

nanohybrid materials. Further, it can serve as a starting point to understand how protein corona can influence the interaction between nanohybrid materials and cells.

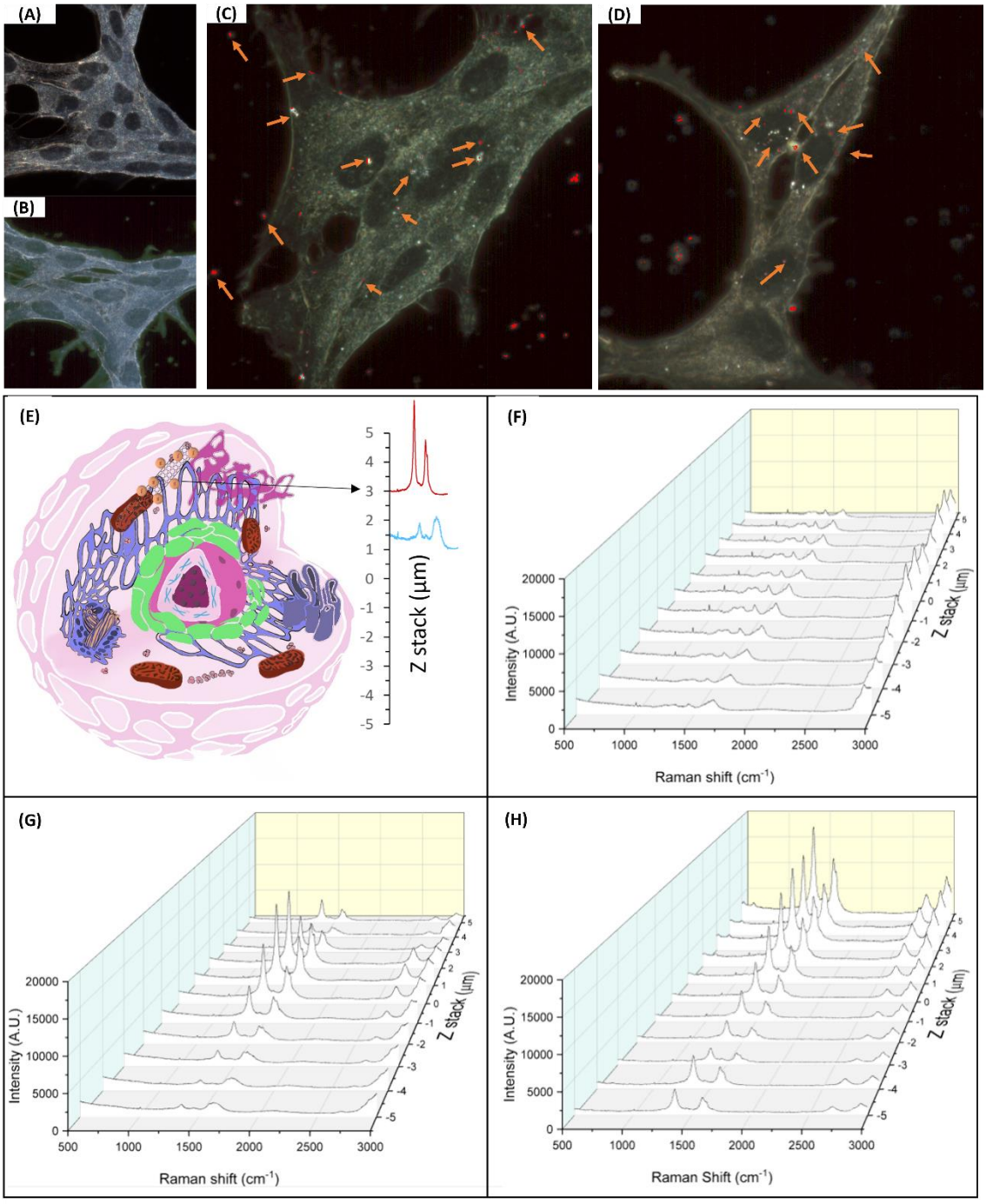

Figure 6. A to D show hyperspectral images of cells (RTG-2) treated with 1 mg L^{-1} of TiO_2-MWCNT; (A) Control cells in DMEM with FBS; (B) Control cells in DMEM without FBS; (C) TiO_2-MWCNT in DMEM media with FBS and (D) TiO_2-MWCNT without FBS. Red dots indicate the location of the nanomaterial in the cells (Point by the orange arrows. Images captured with 100x objective. E-H shows Raman spectral analysis of RTG-2 cells treated with 1 mg L^{-1} of TiO_2-MWCNT; (E) Cell representation of the Raman spectra analysis, where cell was divided in 10 um and laser capture Raman spectra every 1 um step. (F) Z-axis intensity map of a control cell, (G) cell exposed to TiO_2-

MWCNT with SFB and (H) without SFB. Bands used for the map: 1350 cm^{-1} for the D-band and 1580 cm^{-1} for the G-band.

4. Conclusion

In summary, *in vitro* assays with the RTG-2 cell line showed absence of toxicity to TiO_2-MWCNT nanohybrid up to 100 mg mL^{-1}. Furthermore, it was observed that FBS-protein corona on TiO_2-MWCNT had a different profile when compared to MWCNT and TiO_2 nanoparticles. Cryo-TEM images confirmed that TiO_2 has attached to the nanotube surface after incubation with cell culture medium and FBS-protein corona formation. Exploring two complementary advanced optical microscopy techniques (CytoViva and Raman), it was possible to observe that this nanohybrid adheres to the cell membrane in the presence and absence of FBS in the culture medium. The internalisation of nanohybrid was evident when coated with FBS proteins. Finally, this study showed the potential of the RTG-2 cell line as a convenient model for a screening approach for hazards and given the current interest in TiO_2-MWCNT for a range of novel applications, we highlight the potential for this material, as it indicates low toxicity, based on short-term cellular viability test.

Declaration of Competing Interest

The authors declare that they have no known competing financial interests or personal relationships that could have appeared to influence the work reported in this paper.

Acknowledgments

The authors are grateful to the financial support of the Government of Ireland International Education Scholarship (GOI-IES), the National Council for Scientific and Technological Development (CNPq) and for the Coordenação de Aperfeiçoamento de Pessoal de Nível Superior (CAPES/Brasil) finance code 001, INCT-Inomat, and National System of Laboratories on Nanotechnologies (SisNANO/MCTIC). The authors also thank the CNPEM open-facilities (Cryo-TEM and NANOTOX) for the research support.

References

569 Abbas, N., Shao, G.N., Haider, M.S., Imran, S.M., Park, S.S., Jeon, S.-J., Kim, H.T.,
570 2016. Inexpensive sol-gel synthesis of multiwalled carbon nanotube-TiO2 hybrids
571 for high performance antibacterial materials. Materials Science and Engineering: C
572 68, 780–788. https://doi.org/10.1016/j.msec.2016.07.036

573 Ahmadi, M., Ramezani Motlagh, H., Jaafarzadeh, N., Mostoufi, A., Saeedi, R.,
574 Barzegar, G., Jorfi, S., 2017. Enhanced photocatalytic degradation of tetracycline
575 and real pharmaceutical wastewater using MWCNT/TiO2 nano-composite. J
576 Environ Manage 186, 55–63. https://doi.org/10.1016/j.jenvman.2016.09.088

577 Allegri, M., Perivoliotis, D.K., Bianchi, M.G., Chiu, M., Pagliaro, A., Koklioti, M.A.,
578 Trompeta, A.-F.A., Bergamaschi, E., Bussolati, O., Charitidis, C.A., 2016.
579 Toxicity determinants of multi-walled carbon nanotubes: The relationship between
580 functionalization and agglomeration. Toxicol Rep 3, 230–243.
581 https://doi.org/10.1016/J.TOXREP.2016.01.011

582 Alnasser, F., Castagnola, V., Boselli, L., Esquivel-Gaon, M., Efeoglu, E., McIntyre, J.,
583 Byrne, H.J., Dawson, K.A., 2019. Graphene Nanoflake Uptake Mediated by
584 Scavenger Receptors. Nano Lett 19, 1260–1268.
585 https://doi.org/10.1021/acs.nanolett.8b04820

586 Belkhanchi, H., Ziat, Y., Hammi, M., Laghlimi, C., Moutcine, A., Benyounes, A.,
587 Kzaiber, F., 2021. Nitrogen doped carbon nanotubes grafted TiO2 rutile nanofilms:
588 Promising material for dye sensitized solar cell application. Optik (Stuttg) 229,
589 166234. https://doi.org/10.1016/j.ijleo.2020.166234

590 Belkhanchi, H., Ziat, Y., Hammi, M., Laghlimi, C., Moutcine, A., Benyounes, A.,
591 Kzaiber, F., 2020. Synthesis of N-CNT/TiO 2 composites thin films: surface
592 analysis and optoelectronic properties. E3S Web of Conferences 183, 05002.
593 https://doi.org/10.1051/e3sconf/202018305002

594 Bermejo-Nogales, A., Fernández-Cruz, M.L., Navas, J.M., 2017. Fish cell lines as a tool
595 for the ecotoxicity assessment and ranking of engineered nanomaterials.
596 Regulatory Toxicology and Pharmacology 90, 297–307.
597 https://doi.org/10.1016/j.yrtph.2017.09.029

598 Bols, N.C., Dayeh, V.R., Lee, L.E.J., Schirmer, K., 2005. Chapter 2 Use of fish cell
599 lines in the toxicology and ecotoxicology of fish. Piscine cell lines in
600 environmental toxicology, in: Biochemistry and Molecular Biology of Fishes. pp.
601 43–84. https://doi.org/10.1016/S1873-0140(05)80005-0

602 Borgognoni, C.F., Mormann, M., Qu, Y., Schäfer, M., Langer, K., Öztürk, C., Wagner,
603 S., Chen, C., Zhao, Y., Fuchs, H., Riehemann, K., 2015. Reaction of human
604 macrophages on protein corona covered TiO2 nanoparticles. Nanomedicine 11,
605 275–282. https://doi.org/10.1016/J.NANO.2014.10.001

606 Breznan, D., Das, D., MacKinnon-Roy, C., Simard, B., Kumarathasan, P., Vincent, R.,
607 2015. Non-specific interaction of carbon nanotubes with the resazurin assay
608 reagent: Impact on in vitro assessment of nanoparticle cytotoxicity. Toxicology in
609 Vitro 29, 142–147. https://doi.org/10.1016/J.TIV.2014.09.009

Cai, K., Hou, Y., Hu, Y., Zhao, L., Luo, Z., Shi, Y., Lai, M., Yang, W., Liu, P., 2011. Correlation of the Cytotoxicity of TiO2 Nanoparticles with Different Particle Sizes on a Sub-200-nm Scale. Small 7, 3026–3031. https://doi.org/10.1002/smll.201101170

Casado, M., Macken, A., Byrne, H., 2013. Ecotoxicological assessment of silica and polystyrene nanoparticles assessed by a multitrophic test battery. Environ Int.

Casey, A., Herzog, E., Davoren, M., Lyng, F.M., Byrne, H.J., Chambers, G., 2007. Spectroscopic analysis confirms the interactions between single walled carbon nanotubes and various dyes commonly used to assess cytotoxicity. Carbon N Y 45, 1425–1432. https://doi.org/10.1016/J.CARBON.2007.03.033

Castaño, A., Cantarino, M.J., Castillo, P., Tarazona, J.V., 1996. Correlations between the RTG-2 cytotoxicity test EC50 and in vivo LC50 rainbow trout bioassay. Chemosphere 32, 2141–2157. https://doi.org/10.1016/0045-6535(96)00126-9

Cendrowski, K., Jedrzejczak, M., Peruzynska, M., Dybus, A., Drozdzik, M., Mijowska, E., 2014. Preliminary study towards photoactivity enhancement using a biocompatible titanium dioxide/carbon nanotubes composite. J Alloys Compd 605, 173–178. https://doi.org/10.1016/j.jallcom.2014.03.112

Chang, H., Wang, Q., Meng, X., Chen, X., Deng, Y., Li, L., Yang, Y., Song, G., Jia, H., 2022. Effect of Titanium Dioxide Nanoparticles on Mammalian Cell Cycle *In Vitro* : A Systematic Review and Meta-Analysis. Chem Res Toxicol 35, 1435–1456. https://doi.org/10.1021/acs.chemrestox.1c00402

Chen, H., Yang, S., Yu, K., Ju, Y., Sun, C., 2011. Effective Photocatalytic Degradation of Atrazine over Titania-Coated Carbon Nanotubes (CNTs) Coupled with Microwave Energy. J Phys Chem A 115, 3034–3041. https://doi.org/10.1021/jp109948n

Chen, R., Lan, G., Wang, N., Yan, W., Yi, J., Wei, W., 2022. Highly sensitive fiber-optic SPR sensor with surface coated TiO_2 /MWCNT composite film for hydrogen sulfide gas detection. J Phys D Appl Phys 55, 105108. https://doi.org/10.1088/1361-6463/ac378f

da Cruz Schneid, A., Albuquerque, L.J.C., Mondo, G.B., Ceolin, M., Picco, A.S., Cardoso, M.B., 2022. Colloidal stability and degradability of silica nanoparticles in biological fluids: a review. J Solgel Sci Technol. https://doi.org/10.1007/s10971-021-05695-8

Da Dalt, S., Alves, A.K., Bergmann, C.P., 2013. Photocatalytic degradation of methyl orange dye in water solutions in the presence of MWCNT/TiO2 composites. Mater Res Bull 48, 1845–1850. https://doi.org/10.1016/j.materresbull.2013.01.022

Da Silva, G.H., Clemente, Z., Khan, L.U., Coa, F., Neto, L.L.R., Carvalho, H.W.P., Castro, V.L., Martinez, D.S.T., Monteiro, R.T.R., 2018. Toxicity assessment of TiO2-MWCNT nanohybrid material with enhanced photocatalytic activity on Danio rerio (Zebrafish) embryos. Ecotoxicol Environ Saf 165, 136–143. https://doi.org/10.1016/j.ecoenv.2018.08.093

Darbari, S., Abdi, Y., Haghighi, F., Mohajerzadeh, S., Haghighi, N., 2011. Investigating the antifungal activity of TiO 2 nanoparticles deposited on branched carbon nanotube arrays. J Phys D Appl Phys 44, 245401. https://doi.org/10.1088/0022-3727/44/24/245401

Das, D., Sabaraya, I.V., Zhu, T., Sabo-Attwood, T., Saleh, N.B., 2018. Aggregation Behavior of Multiwalled Carbon Nanotube-Titanium Dioxide Nanohybrids: Probing the Part-Whole Question. Environ Sci Technol 52, 8233–8241. https://doi.org/10.1021/acs.est.7b05826

Das, S., Chakraborty, K., Ghosh, D., Pulimi, M., Chandrasekaran, N., Anand, S., Rai, P.K., Mukherjee, A., 2022. Systematic assessment of f-MWCNT transport in aqueous medium: the effect of shear and non-shear forces. International Journal of Environmental Science and Technology. https://doi.org/10.1007/s13762-022-04295-5

David, M.E., Ion, R.M., Grigorescu, R.M., Iancu, L., Holban, A.M., Iordache, F., Nicoara, A.I., Alexandrescu, E., Somoghi, R., Teodorescu, S., Gheboianu, A.I., 2022. Biocompatible and Antimicrobial Cellulose Acetate-Collagen Films Containing MWCNTs Decorated with TiO2 Nanoparticles for Potential Biomedical Applications. Nanomaterials 12, 239. https://doi.org/10.3390/nano12020239

de Medeiros, A.M.Z., Khan, L.U., da Silva, G.H., Ospina, C.A., Alves, O.L., de Castro, V.L., Martinez, D.S.T., 2021. Graphene oxide-silver nanoparticle hybrid material: an integrated nanosafety study in zebrafish embryos. Ecotoxicol Environ Saf 209, 111776. https://doi.org/10.1016/j.ecoenv.2020.111776

Dhenge, S.A., Gade, N.E., Mishra, O.P., Kumar, A., Khandait, V.N., 2020. In vitro Cytotoxicity Analysis of Hybrid Graphene Oxide (hGO) Nano Structures in Caprine Wharton's Jelly Derived Mesenchymal Stem Cells (WJ-MSCs). Indian J Anim Res. https://doi.org/10.18805/ijar.B-3992

Di Ianni, E., Erdem, J.S., Møller, P., Sahlgren, N.M., Poulsen, S.S., Knudsen, K.B., Zienolddiny, S., Saber, A.T., Wallin, H., Vogel, U., Jacobsen, N.R., 2021. In vitro-in vivo correlations of pulmonary inflammogenicity and genotoxicity of MWCNT. Part Fibre Toxicol 18, 25. https://doi.org/10.1186/s12989-021-00413-2

Ding, L., Stilwell, J., Zhang, T., Elboudwarej, O., Jiang, H., Selegue, J.P., Cooke, P.A., Gray, J.W., Chen, F.F., 2005. Molecular Characterization of the Cytotoxic Mechanism of Multiwall Carbon Nanotubes and Nano-Onions on Human Skin Fibroblast. Nano Lett 5, 2448–2464. https://doi.org/10.1021/nl051748o

Docter, D., Distler, U., Storck, W., Kuharev, J., Wünsch, D., Hahlbrock, A., Knauer, S.K., Tenzer, S., Stauber, R.H., 2014. Quantitative profiling of the protein coronas that form around nanoparticles. Nat Protoc 9, 2030–2044. https://doi.org/10.1038/nprot.2014.139

Du, P., Zhao, J., Mashayekhi, H., Xing, B., 2014. Adsorption of Bovine Serum Albumin and Lysozyme on Functionalized Carbon Nanotubes. The Journal of Physical Chemistry C 118, 22249–22257. https://doi.org/10.1021/jp5044943

693 Fent, K., 2001. Fish cell lines as versatile tools in ecotoxicology: assessment of
694 cytotoxicity, cytochrome P4501A induction potential and estrogenic activity of
695 chemicals and environmental samples. Toxicology in Vitro 15, 477–488.
696 https://doi.org/10.1016/S0887-2333(01)00053-4

697 Forest, V., 2022. Experimental and Computational Nanotoxicology—Complementary
698 Approaches for Nanomaterial Hazard Assessment. Nanomaterials 12, 1346.
699 https://doi.org/10.3390/nano12081346

700 Franqui, L.S., De Farias, M.A., Portugal, R. V., Costa, C.A.R., Domingues, R.R., Souza
701 Filho, A.G., Coluci, V.R., Leme, A.F.P., Martinez, D.S.T., 2019. Interaction of
702 graphene oxide with cell culture medium: Evaluating the fetal bovine serum
703 protein corona formation towards in vitro nanotoxicity assessment and
704 nanobiointeractions. Materials Science and Engineering: C 100, 363–377.
705 https://doi.org/10.1016/J.MSEC.2019.02.066

706 Galbis-Martínez, L., Fernández-Cruz, M.L., Alte, L., Valdehita, A., Rucandio, I.,
707 Navas, J.M., 2018. Development of a new tool for the long term in vitro
708 ecotoxicity testing of nanomaterials using a rainbow-trout cell line (RTL-W1).
709 Toxicology in Vitro 50, 305–317. https://doi.org/10.1016/J.TIV.2018.04.007

710 Garvas, M., Testen, A., Umek, P., Gloter, A., Koklic, T., Strancar, J., 2015. Protein
711 Corona Prevents TiO2 Phototoxicity. PLoS One 10, e0129577.
712 https://doi.org/10.1371/journal.pone.0129577

713 Gea, M., Bonetta, Sara, Iannarelli, L., Giovannozzi, A.M., Maurino, V., Bonetta, Silvia,
714 Hodoroaba, V.-D., Armato, C., Rossi, A.M., Schilirò, T., 2019. Shape-engineered
715 titanium dioxide nanoparticles (TiO2-NPs): cytotoxicity and genotoxicity in
716 bronchial epithelial cells. Food and Chemical Toxicology 127, 89–100.
717 https://doi.org/10.1016/j.fct.2019.02.043

718 Ghartavol, H.M., Mohammadi, M.R., Afshar, A., Li, Y., 2019. On the assessment of
719 incorporation of CNT–TiO 2 core–shell structures into nanoparticle TiO 2
720 photoanodes in dye-sensitized solar cells. Photochemical & Photobiological
721 Sciences 18, 1840–1850. https://doi.org/10.1039/C9PP00100J

722 Goswami, M., Yashwanth, B.S., Trudeau, V., Lakra, W.S., 2022. Role and relevance of
723 fish cell lines in advanced in vitro research. Mol Biol Rep 49, 2393–2411.
724 https://doi.org/10.1007/s11033-021-06997-4

725 Guler, M.O., Cetinkaya, T., Uysal, M., Akbulut, H., 2015. High efficiency TiO_2
726 /MWCNT based anode electrodes for Li-ion batteries. Int J Energy Res 39, 172–
727 180. https://doi.org/10.1002/er.3220

728 Hamid, S.B.A., Tan, T.L., Lai, C.W., Samsudin, E.M., 2014. Multiwalled carbon
729 nanotube/TiO2 nanocomposite as a highly active photocatalyst for
730 photodegradation of Reactive Black 5 dye. Chinese Journal of Catalysis 35, 2014–
731 2019. https://doi.org/10.1016/S1872-2067(14)60210-2

732 Hamilton, R.F., Wu, Z., Mitra, S., Shaw, P.K., Holian, A., 2013. Effect of MWCNT
733 size, carboxylation, and purification on in vitro and in vivo toxicity, inflammation

and lung pathology. Part Fibre Toxicol 10, 57. https://doi.org/10.1186/1743-8977-10-57

Hemalatha, K., Ette, P.M., Madras, G., Ramesha, K., 2015. Visible light assisted photocatalytic degradation of organic dyes on TiO2–CNT nanocomposites. J Solgel Sci Technol 73, 72–82. https://doi.org/10.1007/s10971-014-3496-0

Hernández-Alonso, M.D., Fresno, F., Suárez, S., Coronado, J.M., 2009. Development of alternative photocatalysts to TiO2: Challenges and opportunities. Energy Environ Sci 2, 1231. https://doi.org/10.1039/b907933e

Hernández-Moreno, D., Blázquez, M., Navas, J., Fernández-Cruz, M., 2022. Fish cell lines as screening tools to predict acute toxicity to fish of biocidal active substances and their relevant environmental metabolites. Aquatic Toxicology 242, 106020. https://doi.org/10.1016/j.aquatox.2021.106020

Huang, S., Chueh, P.J., Lin, Y.-W., Shih, T.-S., Chuang, S.-M., 2009. Disturbed mitotic progression and genome segregation are involved in cell transformation mediated by nano-TiO2 long-term exposure. Toxicol Appl Pharmacol 241, 182–194. https://doi.org/10.1016/j.taap.2009.08.013

Jones, C.F., Grainger, D.W., 2009. In vitro assessments of nanomaterial toxicity. Adv Drug Deliv Rev 61, 438–456. https://doi.org/10.1016/j.addr.2009.03.005

Klingelfus, T., Disner, G.R., Voigt, C.L., Alle, L.F., Cestari, M.M., Leme, D.M., 2019. Nanomaterials induce DNA-protein crosslink and DNA oxidation: A mechanistic study with RTG-2 fish cell line and Comet assay modifications. Chemosphere 215, 703–709. https://doi.org/10.1016/j.chemosphere.2018.10.118

Kolarova, J., Velisek, J., Svobodova, Z., 2021. Comparison of in vitro (fish cell line) and in vivo (fish and crustacean) acute toxicity tests in aquatic toxicology. Vet Med (Praha) 66, 350–355. https://doi.org/10.17221/161/2020-VETMED

Kyriakidou, K., Brasinika, D., Trompeta, A.F.A., Bergamaschi, E., Karoussis, I.K., Charitidis, C.A., 2020. In vitro cytotoxicity assessment of pristine and carboxyl-functionalized MWCNTs. Food and Chemical Toxicology 141, 111374. https://doi.org/10.1016/j.fct.2020.111374

Lee, T.Y., Alegaonkar, P.S., Yoo, J.-B., 2007. Fabrication of dye sensitized solar cell using TiO2 coated carbon nanotubes. Thin Solid Films 515, 5131–5135. https://doi.org/10.1016/j.tsf.2006.10.056

Lesniak, A., Fenaroli, F., Monopoli, M.P., Åberg, C., Dawson, K.A., Salvati, A., 2012. Effects of the Presence or Absence of a Protein Corona on Silica Nanoparticle Uptake and Impact on Cells. ACS Nano 6, 5845–5857. https://doi.org/10.1021/nn300223w

Long, J., Li, X., Kang, Y., Ding, Y., Gu, Z., Cao, Y., 2018a. Internalization, cytotoxicity, oxidative stress and inflammation of multi-walled carbon nanotubes in human endothelial cells: Influence of pre-incubation with bovine serum albumin. RSC Adv 8, 9253–9260. https://doi.org/10.1039/c8ra00445e

Long, J., Li, X., Kang, Y., Ding, Y., Gu, Z., Cao, Y., 2018b. Internalization, cytotoxicity, oxidative stress and inflammation of multi-walled carbon nanotubes in human endothelial cells: influence of pre-incubation with bovine serum albumin. RSC Adv 8, 9253–9260. https://doi.org/10.1039/C8RA00445E

Longhin, E.M., el Yamani, N., Rundén-Pran, E., Dusinska, M., 2022. The alamar blue assay in the context of safety testing of nanomaterials. Frontiers in Toxicology 4. https://doi.org/10.3389/ftox.2022.981701

Lundqvist, M., Stigler, J., Cedervall, T., Berggård, T., Flanagan, M.B., Lynch, I., Elia, G., Dawson, K., 2011. The Evolution of the Protein Corona around Nanoparticles: A Test Study. ACS Nano 5, 7503–7509. https://doi.org/10.1021/nn202458g

Lungu-Mitea, S., Oskarsson, A., Lundqvist, J., 2018. Development of an oxidative stress in vitro assay in zebrafish (Danio rerio) cell lines. Sci Rep 8, 12380. https://doi.org/10.1038/s41598-018-30880-1

Machado, T.R., Leite, I.S., Inada, N.M., Li, M.S., da Silva, J.S., Andrés, J., Beltrán-Mir, H., Cordoncillo, E., Longo, E., 2019. Designing biocompatible and multicolor fluorescent hydroxyapatite nanoparticles for cell-imaging applications. Mater Today Chem 14, 100211. https://doi.org/10.1016/j.mtchem.2019.100211

Martinez, D.S.T., Da Silva, G.H., de Medeiros, A.M.Z., Khan, L.U., Papadiamantis, A.G., Lynch, I., 2020. Effect of the Albumin Corona on the Toxicity of Combined Graphene Oxide and Cadmium to Daphnia magna and Integration of the Datasets into the NanoCommons Knowledge Base. Nanomaterials 10, 1936. https://doi.org/10.3390/nano10101936

Martins, C.H.Z., Côa, F., da Silva, G.H., Bettini, J., de Farias, M.A., Portugal, R.V., Umbuzeiro, G. de A., Alves, O.L., Martinez, D.S.T., 2022. Functionalization of carbon nanotubes with bovine plasma biowaste by forming a protein corona enhances copper removal from water and ecotoxicity mitigation. Environ Sci Nano 9, 2887–2905. https://doi.org/10.1039/D2EN00145D

Mihalchik, A.L., Ding, W., Porter, D.W., McLoughlin, C., Schwegler-Berry, D., Sisler, J.D., Stefaniak, A.B., Snyder-Talkington, B.N., Cruz-Silva, R., Terrones, M., Tsuruoka, S., Endo, M., Castranova, V., Qian, Y., 2015a. Effects of nitrogen-doped multi-walled carbon nanotubes compared to pristine multi-walled carbon nanotubes on human small airway epithelial cells. Toxicology 333, 25–36. https://doi.org/10.1016/j.tox.2015.03.008

Mihalchik, A.L., Ding, W., Porter, D.W., McLoughlin, C., Schwegler-Berry, D., Sisler, J.D., Stefaniak, A.B., Snyder-Talkington, B.N., Cruz-Silva, R., Terrones, M., Tsuruoka, S., Endo, M., Castranova, V., Qian, Y., 2015b. Effects of nitrogen-doped multi-walled carbon nanotubes compared to pristine multi-walled carbon nanotubes on human small airway epithelial cells. Toxicology 333, 25–36. https://doi.org/10.1016/j.tox.2015.03.008

Mombeshora, E.T., Muchuweni, E., Davies, M.L., Nyamori, V.O., Martincigh, B.S., 2022. Metal-organic chemical vapor deposition of anatase titania on multiwalled

carbon nanotubes for electrochemical capacitors. Energy Sci Eng. https://doi.org/10.1002/ese3.1234

Monopoli, M.P., Åberg, C., Salvati, A., Dawson, K.A., 2012. Biomolecular coronas provide the biological identity of nanosized materials. Nat Nanotechnol 7, 779–786. https://doi.org/10.1038/nnano.2012.207

Morozesk, M., Franqui, L.S., Mansano, A.S., Martinez, D.S.T., Fernandes, M.N., 2018. Interactions of oxidized multiwalled carbon nanotube with cadmium on zebrafish cell line: The influence of two co-exposure protocols on in vitro toxicity tests. Aquatic Toxicology 200, 136–147. https://doi.org/10.1016/j.aquatox.2018.05.002

Morozesk, M., Franqui, L.S., Pinheiro, F.C., Nóbrega, J.A., Martinez, D.S.T., Fernandes, M.N., 2020. Effects of multiwalled carbon nanotubes co-exposure with cadmium on zebrafish cell line: Metal uptake and accumulation, oxidative stress, genotoxicity and cell cycle. Ecotoxicol Environ Saf 202, 110892. https://doi.org/10.1016/J.ECOENV.2020.110892

Muduli, S., Lee, W., Dhas, V., Mujawar, S., Dubey, M., Vijayamohanan, K., Han, S.-H., Ogale, S., 2009. Enhanced Conversion Efficiency in Dye-Sensitized Solar Cells Based on Hydrothermally Synthesized TiO_2 −MWCNT Nanocomposites. ACS Appl Mater Interfaces 1, 2030–2035. https://doi.org/10.1021/am900396m

Munari, M., Sturve, J., Frenzilli, G., Sanders, M.B., Brunelli, A., Marcomini, A., Nigro, M., Lyons, B.P., 2014. Genotoxic effects of CdS quantum dots and Ag 2 S nanoparticles in fish cell lines (RTG-2). Mutation Research/Genetic Toxicology and Environmental Mutagenesis 775–776, 89–93. https://doi.org/10.1016/j.mrgentox.2014.09.003

Naha, P.C., Byrne, H.J., 2013. Generation of intracellular reactive oxygen species and genotoxicity effect to exposure of nanosized polyamidoamine (PAMAM) dendrimers in PLHC-1 cells in vitro. Aquatic Toxicology 132–133, 61–72. https://doi.org/10.1016/j.aquatox.2013.01.020

Naha, P.C., Davoren, M., Casey, A., Byrne, H.J., 2009. An Ecotoxicological Study of Poly(amidoamine) Dendrimers-Toward Quantitative Structure Activity Relationships. Environ Sci Technol 43, 6864–6869. https://doi.org/10.1021/es901017v

Nasr, M., Eid, C., Habchi, R., Miele, P., Bechelany, M., 2018. Recent Progress on Titanium Dioxide Nanomaterials for Photocatalytic Applications. ChemSusChem 11, 3023–3047. https://doi.org/10.1002/cssc.201800874

Natarajan, L., Jenifer, M.A., Mukherjee, A., 2021. Eco-corona formation on the nanomaterials in the aquatic systems lessens their toxic impact: A comprehensive review. Environ Res 194, 110669. https://doi.org/10.1016/j.envres.2020.110669

Nel, A.E., Mädler, L., Velegol, D., Xia, T., Hoek, E.M. V., Somasundaran, P., Klaessig, F., Castranova, V., Thompson, M., 2009. Understanding biophysicochemical interactions at the nano–bio interface. Nat Mater 8, 543–557. https://doi.org/10.1038/nmat2442

Olowoyo, J.O., Kumar, M., Jain, S.L., Babalola, J.O., Vorontsov, A. V., Kumar, U., 2019. Insights into Reinforced Photocatalytic Activity of the CNT–TiO 2 Nanocomposite for CO 2 Reduction and Water Splitting. The Journal of Physical Chemistry C 123, 367–378. https://doi.org/10.1021/acs.jpcc.8b07894

Orge, C.A., Soares, O.S.G.P., Faria, J.L., Pereira, M.F.R., 2017. Synthesis of TiO2-Carbon Nanotubes through ball-milling method for mineralization of oxamic acid (OMA) by photocatalytic ozonation. J Environ Chem Eng 5, 5599–5607. https://doi.org/10.1016/J.JECE.2017.10.030

Parsai, T., Kumar, A., 2019. Understanding effect of solution chemistry on heteroaggregation of zinc oxide and copper oxide nanoparticles. Chemosphere 235, 457–469. https://doi.org/10.1016/j.chemosphere.2019.06.171

Paula, A.J., Silveira, C.P., Martinez, D.S.T., Souza Filho, A.G., Romero, F. V., Fonseca, L.C., Tasic, L., Alves, O.L., Durán, N., 2014. Topography-driven bionano-interactions on colloidal silica nanoparticles. ACS Appl Mater Interfaces 6, 3437–3447. https://doi.org/10.1021/am405594q

Petry, R., Saboia, V.M., Franqui, L.S., Holanda, C. de A., Garcia, T.R.R., de Farias, M.A., de Souza Filho, A.G., Ferreira, O.P., Martinez, D.S.T., Paula, A.J., 2019. On the formation of protein corona on colloidal nanoparticles stabilized by depletant polymers. Materials Science and Engineering: C 105, 110080. https://doi.org/10.1016/j.msec.2019.110080

Posati, T., Bellezza, F., Tarpani, L., Perni, S., Latterini, L., Marsili, V., Cipiciani, A., 2012. Selective internalization of ZnAl-HTlc nanoparticles in normal and tumor cells. A study of their potential use in cellular delivery. Appl Clay Sci 55, 62–69. https://doi.org/10.1016/j.clay.2011.10.006

Quevedo, A.C., Lynch, I., Valsami-Jones, E., 2021. Silver nanoparticle induced toxicity and cell death mechanisms in embryonic zebrafish cells. Nanoscale 13, 6142–6161. https://doi.org/10.1039/D0NR09024G

Runa, S., Lakadamyali, M., Kemp, M.L., Payne, C.K., 2017. TiO_2 Nanoparticle-Induced Oxidation of the Plasma Membrane: Importance of the Protein Corona. J Phys Chem B 121, 8619–8625. https://doi.org/10.1021/acs.jpcb.7b04208

Sacchetti, C., Motamedchaboki, K., Magrini, A., Palmieri, G., Mattei, M., Bernardini, S., Rosato, N., Bottini, N., Bottini, M., 2013. Surface Polyethylene Glycol Conformation Influences the Protein Corona of Polyethylene Glycol-Modified Single-Walled Carbon Nanotubes: Potential Implications on Biological Performance. ACS Nano 7, 1974–1989. https://doi.org/10.1021/nn400409h

Saleh, N., Afrooz, A., Bisesi, J., Aich, N., Plazas-Tuttle, J., Sabo-Attwood, T., Saleh, N.B., Afrooz, A.R.M.N., Bisesi, , Joseph H., Aich, N., Plazas-Tuttle, J., Sabo-Attwood, T., 2014. Emergent Properties and Toxicological Considerations for Nanohybrid Materials in Aquatic Systems. Nanomaterials 4, 372–407. https://doi.org/10.3390/nano4020372

Sánchez, M., Guirado, R., Rincón, M.E., 2007. Multiwalled carbon nanotubes embedded in sol–gel derived TiO2 matrices and their use as room temperature gas sensors. Journal of Materials Science: Materials in Electronics 18, 1131–1136. https://doi.org/10.1007/s10854-007-9144-5

Scott, J., Belden, J.B., Minghetti, M., 2021. Applications of the RTgill-W1 Cell Line for Acute Whole-Effluent Toxicity Testing: In Vitro–In Vivo Correlation and Optimization of Exposure Conditions. Environ Toxicol Chem 40, 1050–1061. https://doi.org/10.1002/etc.4947

Sharma, H.K., Sharma, S.K., Vemula, K., Koirala, A.R., Yadav, H.M., Singh, B.P., 2021. CNT facilitated interfacial charge transfer of TiO2 nanocomposite for controlling the electron-hole recombination. Solid State Sci 112, 106492. https://doi.org/10.1016/j.solidstatesciences.2020.106492

Shimizu, Y., Ateia, M., Wang, M., Awfa, D., Yoshimura, C., 2019. Disinfection mechanism of E. coli by CNT-TiO2 composites: Photocatalytic inactivation vs. physical separation. Chemosphere 235, 1041–1049. https://doi.org/10.1016/j.chemosphere.2019.07.006

Siegrist, K.J., Reynolds, S.H., Kashon, M.L., Lowry, D.T., Dong, C., Hubbs, A.F., Young, S.-H., Salisbury, J.L., Porter, D.W., Benkovic, S.A., McCawley, M., Keane, M.J., Mastovich, J.T., Bunker, K.L., Cena, L.G., Sparrow, M.C., Sturgeon, J.L., Dinu, C.Z., Sargent, L.M., 2014. Genotoxicity of multi-walled carbon nanotubes at occupationally relevant doses. Part Fibre Toxicol 11, 6. https://doi.org/10.1186/1743-8977-11-6

Sit, I., Xu, Z., Grassian, V.H., 2019. Plasma protein adsorption on TiO2 nanoparticles: Impact of surface adsorption on temperature-dependent structural changes. Polyhedron 171, 147–154. https://doi.org/10.1016/J.POLY.2019.06.036

Sun, Q., Kanehira, K., Taniguchi, A., 2016. Low doses of TiO_2 -polyethylene glycol nanoparticles stimulate proliferation of hepatocyte cells. Sci Technol Adv Mater 17, 669–676. https://doi.org/10.1080/14686996.2016.1239499

Tedja, R., Lim, M., Amal, R., Marquis, C., 2012. Effects of Serum Adsorption on Cellular Uptake Profile and Consequent Impact of Titanium Dioxide Nanoparticles on Human Lung Cell Lines. ACS Nano 6, 4083–4093. https://doi.org/10.1021/nn3004845

Tenzer, S., Docter, D., Kuharev, J., Musyanovych, A., Fetz, V., Hecht, R., Schlenk, F., Fischer, D., Kiouptsi, K., Reinhardt, C., Landfester, K., Schild, H., Maskos, M., Knauer, S.K., Stauber, R.H., 2013. Rapid formation of plasma protein corona critically affects nanoparticle pathophysiology. Nat Nanotechnol 8, 772–781. https://doi.org/10.1038/nnano.2013.181

Uboldi, C., Urbán, P., Gilliland, D., Bajak, E., Valsami-Jones, E., Ponti, J., Rossi, F., 2016. Role of the crystalline form of titanium dioxide nanoparticles: Rutile, and not anatase, induces toxic effects in Balb/3T3 mouse fibroblasts. Toxicology in Vitro 31, 137–145. https://doi.org/10.1016/j.tiv.2015.11.005

Vevers, W.F., Jha, A.N., 2008. Genotoxic and cytotoxic potential of titanium dioxide (TiO2) nanoparticles on fish cells in vitro. Ecotoxicology 17, 410–420. https://doi.org/10.1007/s10646-008-0226-9

Vijayalakshmi, U., Chellappa, Anjaneyulu, Manivasagam, G., 2015. Preparation and evaluation of the cytotoxic nature of TiO2 nanoparticles by direct contact method. Int J Nanomedicine 31. https://doi.org/10.2147/IJN.S79978

Vranic, S., Gosens, I., Jacobsen, N.R., Jensen, K.A., Bokkers, B., Kermanizadeh, A., Stone, V., Baeza-Squiban, A., Cassee, F.R., Tran, L., Boland, S., 2017. Impact of serum as a dispersion agent for in vitro and in vivo toxicological assessments of TiO2 nanoparticles. Arch Toxicol 91, 353–363. https://doi.org/10.1007/s00204-016-1673-3

W. Oh, Feng-jun Zhang, Ming-liang Chen, 2009. Preparation of MWCNT/TiO2 Composites by Using MWCNTs and Titanium(IV) Alkoxide Precursors in Benzene and their Photocatalytic Effect and Bactericidal Activity. Bull Korean Chem Soc 30, 2637–2642. https://doi.org/10.5012/bkcs.2009.30.11.2637

Wang, J., Fan, Y., 2014. Lung Injury Induced by TiO2 Nanoparticles Depends on Their Structural Features: Size, Shape, Crystal Phases, and Surface Coating. Int J Mol Sci 15, 22258–22278. https://doi.org/10.3390/ijms151222258

Wang, J., Lin, Y., Pinault, M., Filoramo, A., Fabert, M., Ratier, B., Bouclé, J., Herlin-Boime, N., 2015. Single-Step Preparation of TiO_2 /MWCNT Nanohybrid Materials by Laser Pyrolysis and Application to Efficient Photovoltaic Energy Conversion. ACS Appl Mater Interfaces 7, 51–56. https://doi.org/10.1021/am507179c

Wang, X., Xia, T., Ntim, S.A., Ji, Z., George, S., Meng, H., Zhang, H., Castranova, V., Mitra, S., Nel, A.E., 2010. Quantitative Techniques for Assessing and Controlling the Dispersion and Biological Effects of Multiwalled Carbon Nanotubes in Mammalian Tissue Culture Cells. ACS Nano 4, 7241–7252. https://doi.org/10.1021/nn102112b

Wheeler, K.E., Chetwynd, A.J., Fahy, K.M., Hong, B.S., Tochihuitl, J.A., Foster, L.A., Lynch, I., 2021. Environmental dimensions of the protein corona. Nat Nanotechnol 16, 617–629. https://doi.org/10.1038/s41565-021-00924-1

Yoon, C.-J., Lee, S.-H., Kwon, Y.-B., Kim, K., Lee, K.-H., Kim, S.M., Kim, Y.-K., 2021. Fabrication of sustainable and multifunctional TiO2@carbon nanotube nanocomposite fibers. Appl Surf Sci 541, 148332. https://doi.org/10.1016/j.apsusc.2020.148332

Yurdakök-Dikmen, B., Vejselova, D., Kutlu, H.M., Filazi, A., Erkoç, F., 2018. Effects of synthetic pyrethroids on RTG-2 cells. Toxin Rev 37, 304–312. https://doi.org/10.1080/15569543.2017.1366922

Zhang, T., Tang, M., Yao, Y., Ma, Y., Pu, Y., 2019. <p>MWCNT interactions with protein: surface-induced changes in protein adsorption and the impact of protein

corona on cellular uptake and cytotoxicity</p>. Int J Nanomedicine Volume 14, 993–1009. https://doi.org/10.2147/IJN.S191689

Zhang, Ting, Tang, M., Kong, L., Li, H., Zhang, Tao, Zhang, S., Xue, Y., Pu, Y., 2012. Comparison of cytotoxic and inflammatory responses of pristine and functionalized multi-walled carbon nanotubes in RAW 264.7 mouse macrophages. J Hazard Mater 219–220, 203–212. https://doi.org/10.1016/j.jhazmat.2012.03.079

Zhang, Y., Wang, B., Meng, X., Sun, G., Gao, C., 2011a. Influences of Acid-Treated Multiwalled Carbon Nanotubes on Fibroblasts: Proliferation, Adhesion, Migration, and Wound Healing. Ann Biomed Eng 39, 414–426. https://doi.org/10.1007/s10439-010-0151-y

Zhang, Y., Wang, B., Meng, X., Sun, G., Gao, C., 2011b. Influences of Acid-Treated Multiwalled Carbon Nanotubes on Fibroblasts: Proliferation, Adhesion, Migration, and Wound Healing. Ann Biomed Eng 39, 414–426. https://doi.org/10.1007/s10439-010-0151-y

Zhao, X., Jia, Q., Song, N., Zhou, W., Li, Y., 2010. Adsorption of Pb(II) from an aqueous solution by titanium dioxide/carbon nanotube nanocomposites: Kinetics, thermodynamics, and isotherms. J Chem Eng Data 55, 4428–4433. https://doi.org/10.1021/je100586r

Zhou, L., Forman, H.J., Ge, Y., Lunec, J., 2017. Multi-walled carbon nanotubes: A cytotoxicity study in relation to functionalization, dose and dispersion. Toxicology in Vitro 42, 292–298. https://doi.org/10.1016/j.tiv.2017.04.027

Zouzelka, R., Kusumawati, Y., Remzova, M., Rathousky, J., Pauporté, T., 2016. Photocatalytic activity of porous multiwalled carbon nanotube-TiO2 composite layers for pollutant degradation. J Hazard Mater 317, 52–59. https://doi.org/10.1016/J.JHAZMAT.2016.05.056